Neuro-Oncology

XX(XX), 1–10, 2021 | doi:10.1093/neuonc/noab031 | Advance Access date 16 February 2021

# Integrated molecular analysis of adult sonic hedgehog (SHH)-activated medulloblastomas reveals two clinically relevant tumor subsets with VEGFA as potent prognostic indicator

**Andrey Korshunov,[†] Konstantin Okonechnikov,[†] Damian Stichel, Marina Ryzhova, Daniel Schrimpf, Felix Sahm, Philipp Sievers, Oksana Absalyamova, Olga Zheludkova, Andrey Golanov, David T. W. Jones, Stefan M. Pfister, Andreas von Deimling, and Marcel Kool**

*Clinical Cooperation Unit Neuropathology (B300), German Cancer Research Center (DKFZ), Heidelberg, Germany (A.K., D. Stichel, D. Schrimpf, F.S., P.S., A.v.D.); Department of Neuropathology, University of Heidelberg, Heidelberg, Germany (A.K., D. Stichel, D. Schrimpf, F.S., P.S., A.v.D.); Hopp Children's Cancer Center Heidelberg (KiTZ), Heidelberg, Germany (A.K., K.O., F.S., D.T.W.J., S.M.P., M.K.); Division of Pediatric Neuro-oncology, German Cancer Consortium (DKTK) and German Cancer Research Center (DKFZ), Heidelberg, Germany (K.O., S.M.P., M.K.); N.N. Burdenko Neurosurgical Research Centre, Moscow, Russia (M.R., O.A., A.G.); Department of Neuro-Oncology, Russian Scientific Center of Radiology, Moscow, Russia (O.Zh.); Pediatric Glioma Research Group (B360), German Cancer Research Center (DKFZ), Heidelberg, Germany (D.T.W.J.); Department of Pediatric Oncology, Hematology & Immunology, University of Heidelberg, Heidelberg, Germany (S.M.P.); Princess Máxima Center for Pediatric Oncology, Utrecht, the Netherlands (M.K.)*

[†]These authors contributed equally to this work.

**Corresponding Author:** Andrey Korshunov, MD, Clinical Cooperation Unit Neuropathology (B300), German Cancer Research Center (DKFZ), Im Neuenheimer Feld 224, 69120 Heidelberg, Germany; Department of Neuropathology, University Hospital Heidelberg, Im Neuenheimer Feld 224, 69120 Heidelberg, Germany (andrey.korshunov@med.uni-heidelberg.de).

**Abstract**

**Background.** Up to now, adult medulloblastoma (MB) patients are treated according to the protocols elaborated for pediatric MB although these tumors are different in terms of clinical outcomes and biology. Approximately 70% of adult MB disclose a sonic hedgehog (SHH) molecular signature in contrast to about 30% in pediatric cohorts. In addition, adult SHH-MB (aSHH-MB) are clinically heterogeneous but there is consensus neither on their optimal treatment nor on risk stratification. Thus, the identification of clinically relevant molecular subsets of aSHH-MB and identification of potential treatment targets remains inconclusive.

**Methods.** We analyzed 96 samples of institutionally diagnosed aSHH-MB through genome-wide DNA methylation profiling, targeted DNA sequencing, and RNA sequencing to identify molecular subcategories of these tumors and assess their prognostic significance.

**Results.** We defined two aSHH-MB numerically comparable epigenetic subsets with clinical and molecular variability. The subset "aSHH-MBI" (46%/48%) was associated with *PTCH1/SMO* (54%/46%) mutations, "neuronal" transcriptional signatures, and favorable outcomes after combined radio-chemotherapy (5-year PFS = 80% and OS = 92%). The clinically unfavorable "aSHH-MBII" subset (50%/52%; 5-year PFS = 24% and OS = 45%) disclosed *GLI2* amplifications (8%), loss of 10q (22%), and gene expression signatures associated with angiogenesis and embryonal development. aSHH-MBII tumors revealed strong and ubiquitous expression of *VEGFA* both at transcript and protein levels that was correlated with unfavorable outcome.

**Conclusions.** (1) The histologically uniform aSHH-MB cohort exhibits clear molecular heterogeneity separating these tumors into two molecular subsets (aSHH-MBI and aSHH-MBII), which are associated with different

cytogenetics, mutational landscapes, gene expression signatures, and clinical course. (2) VEGFA appears to be a promising biomarker to predict clinical course, which needs further prospective validation as its potential role in the pathogenesis of this subset.

### Key Points

1. There are two clinically distinct aSHH-MB molecular subsets as detected by integrated DNA- and RNA-based analysis.
2. Through VEGFA expression analysis at the mRNA and/or protein level, aSHH-MB patients may be stratified into clinically relevant groups.

### Importance of the Study

Adult medulloblastoma with SHH molecular signature (aSHH-MB) is a rare tumor entity, which is associated with various treatment strategies and clinical outcomes. The identification of clinically relevant molecular subsets of aSHH-MB and potential treatment targets has so far been hindered by the relatively small cohorts analyzed to date. Our study of a comprehensive DNA- and RNA-based analysis of a representative retrospective and uniformly treated aSHH-MB series disclosed two distinct molecular subsets of these tumors and VEGFA as a potent molecular marker, which may help to improve patient stratification.

Medulloblastoma (MB) accounts for 4%-6% of all primary intracranial tumors. It presents primarily in children with 85% of MB being diagnosed in patients below 18 years of age. In contrast, MB is rare in adults and accounts for less than 1% of primary intracranial malignancies in this age group.[1–3] The low incidence of MB in adults, the lack of a common treatment strategy for these patients, and the frequent occurrence of late relapses more than 5 years after primary diagnosis have hindered a systematic analysis of biological and clinical peculiarities of adult MB to date. Moreover, current studies documented differences between childhood and adult tumors with regard to their clinical course and molecular patterns.[3–5] In contrast to pediatric MB, most of the adult tumors disclosed a sonic hedgehog (SHH) molecular signature—70% vs ~30% in pediatric cohorts.[4–7] Additionally, it has been shown that SHH-MB in infants, children, and adults strongly differ in transcriptome, methylome, copy number aberrations, and mutational landscapes including hereditary cancer predisposition.[7–10] DNA/methylation and transcriptome profiling identified four molecular subtypes within SHH-MB with prognostic relevance.[8] SHH-β and SHH-γ MB subtypes occur mostly in infants,[8] are largely overlapping with the infant subtypes iSHH-I and iSHH-II, respectively, and may have a different outcome depending on the therapy that was used for treatment.[9,11] SHH-α MB variant is associated with older children and within this subtype, it is mainly the *TP53* status that determines whether these children have a poor outcome (*TP53* mutated) or good outcome (*TP53* wild type).[8,10,12] In addition, SHH-δ subtype presents mainly in adults.[8–10]

On the other hand, adult SHH-MB (aSHH-MB) are also clinically heterogeneous and disclose various outcomes, but there is consensus neither on their optimal treatment nor on risk stratification.[13–17] Thus, the identification of clinically relevant molecular subsets of aSHH-MB and identification of potential treatment targets for high-risk patients were so far hampered either by the small sample size in previously analyzed cohorts or low frequency of recurrent aberrations and thus remained inconclusive.[18–20] On the other hand, preclinical and early clinical data suggest that aSHH-MB patients may be the best group to benefit from molecularly targeted therapies, for example, from combination of treatment with SMO and/or AKT/mTOR inhibitors including their application in combination with standard radio-chemotherapy in the framework of upfront trials.[5,21]

In the present study, tissue samples from 96 aSHH-MB patients institutionally treated with radio-chemotherapy were subjected to genome-wide analysis combining DNA methylation profiling, targeted next-generation DNA sequencing, and gene expression analysis to identify potential molecular subcategories of these tumors thus assessing their prognostic significance and further clinical application.

## Methods

### Patient Population

Tissue tumor samples with histological diagnosis "MB" obtained from 96 adult patients (age 19-55 years) were analyzed. All 96 tumors were molecularly classified as "SHH MB" (subclass SHH_MB-Adult) according to the "Heidelberg brain tumor classifier; v11b4" (www.molecularneuropathology.org; see Results),[22,23] which

also was matched to recently identified SHH-δ molecular subset.[8] All these patients were uniformly treated in the Burdenko Neurosurgical Institute between January 1, 1998 and January 1, 2018 with surgery and "Hirn Tumor" (HIT)-based protocol of radio-chemotherapy (see Results); they had no clinical history of previously treated tumors. This retrospective study was conducted under the auspices of the Ethics Committee of the Burdenko Neurosurgical Institute (Ethical vote number 563/6-16) and those of the University of Heidelberg, in compliance with the Russian Federation and German rules of the Health Insurance Portability, and in adherence to the tenets of the Declaration of Helsinki. The follow-up analysis was stalled on June 1, 2020 (the endpoint of follow-up).

### DNA Methylation, Targeted Next-Generation Sequencing (NGS), and RNA Sequencing

DNA (96) and RNA (74) were extracted from formalin-fixed and paraffin-embedded (FFPE) tissue samples using the automated Maxwell system (Promega, Madison, WI, USA), according to the manufacturer's instructions.[24] DNA was analyzed using the Illumina Human Methylation 450k or 850k/EPIC BeadChip array as described.[22–24] For unsupervised hierarchical clustering (UCL), we selected the 20 000 most variably methylated probes across the dataset as measured by standard deviation. Additional analysis was performed using a t-distributed stochastic neighbor embedding (t-SNE)-based approach. Copy number profiles were generated using the "conumee" package for R. The Random Forest Classifier was applied for data analysis and detection of tumor calibration scores as described.[22,23]

Targeted NGS with 130 cancer-associated genes was performed using the NextSeq 500 (Illumina) as described.[24] Sequence data were mapped to the reference human genome using the Burrows-Wheeler Aligner and were processed using the publicly available SAM tools.

RNA sequencing was performed on a NextSeq 500 (Illumina) as described.[24] The reads were aligned to hg19 reference using STAR version 2.5.2b and for each sample, gene expression was quantified by the feature counts module of the Subread package version 1.4.6 using Gencode version 19 annotations with considering uniquely mapped reads only.[24] Unsupervised tumor samples comparison was performed with UCL and t-SNE analyses, based on the selection of the top 500 most variable genes with *log2* Reads Per Kilobase Million (RPKM) gene expression normalization. Subgroup-specific differential gene expression analysis was performed by comparing one molecular class against the other using DESeq2 R package (adjusted $P < .05$) and gene ontology analysis was done by combining the top 250 specifically expressed genes in the individual molecular classes, with visualization using ClueGO (Cytoscape) version 3.4.[25] Analyses were performed using R2: Genomics Analysis and Visualization Platform (http://r2.amc.nl). Fusion discovery was done based on RNA sequencing data using five independent algorithms as described.[26] For survival analyses based on *VEGFA* expression, samples were categorized as having "high" and "low" mRNA levels using a cutoff in expression that resulted in the lowest log-rank *P* value using a Bonferroni correction for multiple testing.

### Immunohistochemistry (IHC) With VEGFA Antibody

IHC was conducted on 4-µm thick FFPE tissue sections mounted on adhesive slides followed by drying at 80°C for 15 min. For IHC analysis of VEGFA protein, a mouse monoclonal antibody (clone VG1; MA5-12184, Thermo Fisher Scientific Inc.) was applied. IHC was performed with an automated immunostainer (Benchmark; Ventana XT) using antigen-retrieval protocol CC1 and a working antibody dilution of 1:100 with incubation at 37°C for 32 min.

### Statistics

The distribution of progression-free survival and overall survival (PFS and OS, respectively) was calculated according to the Kaplan-Meier method. For multivariate analysis, Cox proportional hazards regression models were used. Estimated hazard ratios are provided with 95% confidence intervals and a *P* value from the Wald test. Tests with a *P* value below .05 were considered significant.

## Results

### Clinical and Pathological Characteristics of the aSHH-MB Cohort

Clinical characteristics from 96 patients with aSHH-MB included in the current study are outlined in Table 1 and Supplementary Table 1. Tumors occurred predominately in young adults (range 19-55 years; median 28 years), with the vast majority of patients (65%) between 20 and 40 years. There was a significant preponderance of male patients in this cohort (64% vs 36% for female; male:female ratio 2.2:1). Fifty-one tumors (53%) were located laterally affecting the cerebellar hemisphere only, whereas the other 45 MBs (47%) occupied the vermis and both neighboring hemispheres. Only 15 (16%) patients displayed neuroradiological patterns of tumor dissemination at initial presentation (M2-3). Gross total tumor (GTR) resection was achieved in 65 patients (68%). All patients were treated with HIT-based protocol of radio-chemotherapy: craniospinal irradiation (CSI; with 36 Gy to the neuroaxis and 56 Gy to the primary tumor site) and 6-8 cycles of maintenance chemotherapy including vincristine, lomustine (CCNU), and cisplatin. According to histopathological criteria defined by the current WHO classification,[27] all 96 tumors were diagnosed as nodular/desmoplastic MB composed of two "prototypic" components: nodular reticulin-free zones ("pale islands"), and interstitial, reticulin-rich foci (Figure 1A).

Follow-up data were available for all patients (median time of observation = 63 months), demonstrating that

**Table 1** Clinical and Molecular Variables in Different Epigenetic Subgroups of Adult SHH-MB

| Variable | All Cohort (96) | aSHH-MBI (46) | aSHH-MBII (50) | *P*Value[a] |
|---|---|---|---|---|
| Mean age (range) | 30.1 (19-55) | 29.3 (19-55) | 31 (19-48) | NA |
| Age > 30 years | 39%/41% | 18%/40% | 21%/42% | NA |
| Gender (M vs F) | 66% vs 34% | 74% vs 26% | 58% vs 42% | <.01 |
| Location (Lat vs Med) | 53% vs 47% | 52% vs 48% | 54% vs 46% | NA |
| M stage 2-3 | 15%/16% | 5%/11% | 10%/20% | NA |
| Resection (GTR vs NTR) | 68% vs 32% | 67% vs 33% | 68% vs 32% | NA |
| Relapses<br>Local<br>Mixed (Local + MTS)<br>CNS metastases alone<br>CNS + extra-neural MTS | 51%/52%<br>17%/34%<br>15%/28%<br>11%/22%<br>8%/16% | 16%/42%<br>10%/63%<br>4%/25%<br>2%/12%<br>0 | 35%/67%<br>7%/20%<br>11%/30%<br>9%/25%<br>8%/25% | <.01<br><.01<br>NA<br><.01<br><.01 |
| 5-year PFS (months) | 57% | 78% | 22% | <.01 |
| Death | 32%/32% | 5%/11% | 27%/52% | <.01 |
| 5-year OS (months) | 73% | 92% | 42% | <.01 |
| Mean CNVs[b] (range) | 2.46 (0-10) | 2.46 (0-10) | 2.47 (0-8) | NA |
| Balanced profile | 21%/22% | 12%/24% | 9%/20% | NA |
| *GIL2* amplification | 7%/8% | 0 | 7%/14% | <.01 |
| Loss 9q | 30%/31% | 18%/35% | 12%/25% | NA |
| Loss 10q | 12%/13% | 0 | 12%/24% | <.01 |
| Loss 17p | 21%/22% | 5%/11% | 16%/32% | <.01 |
| Loss 14q | 25%/26% | 18%/40% | 7%/14% | <.01 |
| Gain 3q | 24%/24% | 11%/25% | 13%/26% | NA |
| Mean NM[c] (range) | 7.62 (2-21) | 4.81 (2-10) | 10.48 (5-21) | <.01 |
| *PTCH1* mutation | 44%/45% | 25%/54% | 18%/35% | <.01 |
| *SMO* mutation | 30%/31% | 21%/46% | 9%/18% | <.01 |
| *PRKAR1A* mutation | 15%/16% | 0 | 15%/30% | <.01 |
| *pTERT* mutation | 82%/85% | 38%/83% | 44%/88% | NA |
| *VEGFA* expression/ RPKM[d] | 690 (40-8700) | 220 (40-594) | 1010 (70-8700) | <.01 |
| *VEGFA* expression/log2 > 2.5[d] | 33 (45%) | 5 (14%) | 28 (76%) | <.01 |

**Abbreviations:** GTR, gross total tumor; MTS, metastatic; NA, not applicable; NTR, near-total; OS, overall survival; PFS, progression-free survival.
[a]Mann-Whitney *U* test; [b]Copy number variants; [c]Number of mutations; [d]N = 74; RPKM: Reads Per Kilobase Million.

51 (52%) of tumors recurred (median PFS of 50 months) and 32 (33%) of patients died within the follow-up period (median OS of 61 months). Five-year PFS and OS were 57% and 73%, respectively. Seventeen patients with relapsed disease (34%) experienced isolated local tumor regrowth, whereas 33 of remaining relapsed patients (66%) developed metastatic disease progression showing the following patterns (Supplementary Figure 1): (i) spinal metastases (solitary or diffuse; 11%/22%); (ii) intracranial dissemination alone or combined with local tumor recurrence (14%/28%), and (iii) extra-neural dissemination (bone marrow, liver or lymph nodes; 8%/16%). There was no significant association between patients' survival and various clinical variables, including patients' age (<30 vs >30 or <40 vs >40 years), gender, tumor location, M stage at diagnosis, and level of resection (Tables 2 and 3).

## Methylation Profiling Disclosed Two Molecular aSHH-MB Subsets With Different Clinical Outcomes

Cluster analysis of the DNA methylation profiles generated for the adult 96 MB samples was performed, which all fall into the aSHH-MB subgroup as mentioned above. Using consensus UCL and the 20.000 most differentially methylated CpG sites identified two clearly demarcated epigenetic subsets provisionally designated as aSHH-MBI (n = 46/48%) and aSHH-MBII (n = 50/52%) (Figure 1B). These clusters remained mostly stable when using lower numbers of differentially methylated CpG sites (10 000, 5 000, or 1 000; not shown) and were confirmed with t-SNE analysis (Figure 1C).

No significant differences were observed between these two molecular aSHH-MB subsets patient's age,

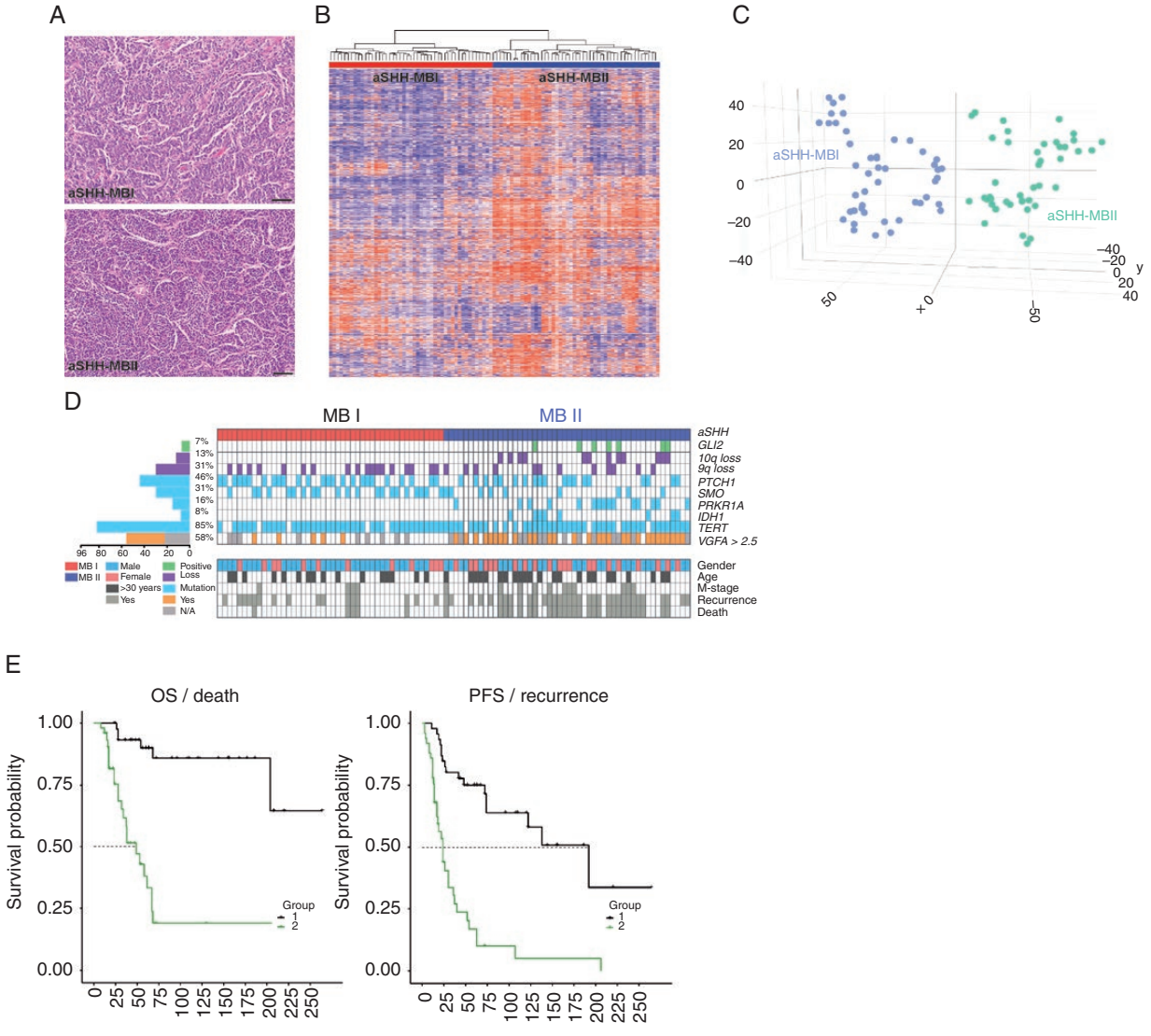


**Fig.1** (A) Both molecular aSHH-MB variants (see B, C) revealed similar histological appearance designated as desmoplastic/nodular MB variant (the scale bars: 50 μm). (B) Unsupervised hierarchical clustering (UCL) of DNA methylation of the full adult SHH MB cohort (n = 96) based on the 20 000 most variable methylation probes (SD > 0.30). Two main epigenetic clusters were identified (aSHH-MBI—red line and aSHH-MBII—blue line). (C) Two-dimensional t-distributed stochastic neighbor embedding (t-SNE) analysis of adult SHH MB also revealed two tumor methylation subgroups—aSHH-MBI (blue spots) and aSHH-MBII (green spots). (D) Oncoprint depicting clinical characteristics, chromosomal aberrations, and driver SHH-activated gene mutations which are differentially distributed in two aSHH-MB subgroups, derived from UCL and t-SNE clustering. (E) Survival analysis for two epigenetic aSHH-MB variants shows that progression-free and overall survival for aSHH-MBII patients (green line) were significantly worse than those for aSHH-MBI patients (black line; log-rank test; $P < .01$).

tumor location, M stage at diagnosis, or microscopic appearance although female patients were more frequent in aSHH-MBII (42% vs 26% for aSHH-MBI; Table 1, Figure 1D). The median number of copy number variations (CNAs) calculated for aSHH-MBI and MBII were similar: 3.86 and 3.87 per tumor, respectively ($P = .84$). Amplification of *GLI2* (7%/8%, accompanied with chromothripsis patterns in 3 samples) and loss of 10q (14%/22%) were only found in aSHH-MBII (Figure 1D, Supplementary Figure 2A–D). Loss of 17p was more frequent in aSHH-MBII (32% vs 11%), whereas loss of 14q (40% vs 14%) was more common in aSHH-MBI subset. Frequency of 9q loss and 3q gain was similar in both aSHH-MB subsets.

Using targeted NGS, somatic single-nucleotide variants (SNVs) and small insertions/deletions were analyzed across all 96 samples studied (Table 1, Figure 1D, Supplementary Table 1). The mean number of alterations for the entire tumor cohort was 7.6 ± 3.2 per tumor. Recurrent mutations affected three "prototypic" SHH-associated genes: *PTCH1* (45%), *SMO* (31%), and *PRKAR1A* (16%), which all were mutually exclusive involving most of aSHH-MB (92%). Frequent mutations of *DDX3X* (35%) and *CREBBP* (20%) were also found; other non-recurrent genetic alterations were scattered throughout the cohort. We detected no *TP53* or *PTEN* mutations in this tumor set. *IDH1* mutations (all R132C) were identified in 8 (8%) cases. The mean number of gene alterations was significantly higher for aSHH-MBII: 10.4 ±

**Table 2** Results of Univariate and Multivariate PFS Analysis for 96 Adult SHH MB

| Variable | Uni-HR | *P*Value[a] | Multi-HR | *P*Value[a] |
|---|---|---|---|---|
| Age: < 35 years vs > 35 years | 0.21 | .86 | 0.42 | .76 |
| Gender: male vs female | 0.27 | .65 | 0.67 | .46 |
| Tumor location: median vs lateral | 0.01 | .91 | 0.17 | .81 |
| M stage: M0-1 vs M2-3 | 4.02 | .08 | 3.53 | .12 |
| Tumor resection: NTR vs GTR | 2.44 | .13 | 1.32 | .59 |
| *GLI2* amplification: yes vs no | **9.72** | **<.01** | 2.88 | .11 |
| Loss 9q: yes vs no | 2.21 | .14 | 1.54 | .34 |
| Loss 10q: yes vs no | **10.6** | **<.01** | 2.78 | .14 |
| Loss 17p: yes vs no | 1.54 | .21 | 1.59 | .22 |
| Loss 14q: yes vs no | 0.58 | .44 | 0.67 | .48 |
| Gain 3q: yes vs no | 0.75 | .38 | 0.91 | .88 |
| Balanced profile: yes vs no | 1.54 | .21 | 1.08 | .91 |
| *PTCH1* mutation: yes vs no | 0.82 | .33 | 1.08 | .91 |
| *SMO* mutation: yes vs no | 0.21 | .17 | 0.38 | .33 |
| *PRKAR1A* mutation: yes vs no | 0.24 | .22 | 0.34 | .47 |
| Molecular group: aSHH-MBII vs MBI | **20.6** | **<.01** | **8.73** | **.01** |

**Abbreviations:** GTR, gross total tumor; NTR, near-total tumor; PFS, progression-free survival.
[a]Log-rank test.
Bold value represent the significant differences.

4.3 in comparison to 4.8 ± 3.3 for aSHH-MBI, respectively (Supplementary Figure 2E; $P < .01$). Also, strong differences in mutational landscapes were found for these aSHH-MB cohorts (Table 1, Figure 1D, Supplementary Table 1). Thus, *PTCH1* and *SMO* mutations prevailed in aSHH-MBI (55% and 30% vs 32% and 8% for SHH-MBII; $P < .01$), but *PRKR1A* and *IDH1* mutations were only detected in the aSHH-MBII subset. *TERT* promoter mutations (*C228T*—96% and *C250T*—4%) were identified in 85% of samples with similar proportions between aSHH-MBI and MBII (83% and 88%, respectively; $P = .81$).

Survival analysis revealed that patients allocated to the aSHH-MBI subset showed a significantly better 5-year PFS (80%) and OS (92%) than those from the aSHH-MBII subset (24% and 45%, respectively; Table 1, Figure 1E). Tumors with aSHH-MBI signatures recurred frequently as late local relapses (70%; PFS—98 months), whereas the vast majority of recurred aSHH-MBII manifested as rapid intra- and extra-neural tumor spread (84%; PFS—21 months). Survival analyses for molecular parameters revealed *GLI2* amplification and loss of 10q as predictors of poor outcomes, whereas aSHH-MBI molecular signature was identified as an independent variable associated with favorable survival (Tables 2 and 3).

## Expression Profiling Disclosed Gene Sets Differentially Activated Between aSHH-MB Methylome Subgroups

In 74 samples, we did RNA sequencing-based gene expression profiling in order to assess transcriptional differences between aSHH-MBI[28] and aSHH-MBII[28] samples. Comparing transcriptome profiles generated for both aSHH-MB subsets we detected 2712 genes and processed pseudogenes differentially expressed between these molecular variants (DESeq2 R algorithm; adjusted *P* value < .05; Supplementary Table 3). A set of the top most-confident 20 genes differentially expressed between two methylome aSHH-MB subsets allowed to discriminate their transcriptome signatures (Figure 2A). We compared epigenetic and RNA sequencing data but we did not find any changes in methylation status for top genes differentially expressed between aSHH-MBI and MBII.

Further, to delineate characteristic biological processes for methylome-derived aSHH-MB subgroups, we performed pathway identification with Gene Ontology analysis (Figure 2B; Supplementary Tables 4 and 5). The transcriptome signatures of aSHH-MBI subset included seven pathways, which were characterized by genes involved in neuronal function, synaptic transmission, membrane invagination, and phagocytosis. In contrast, the transcriptome aSHH-MBII profiles involved 38 signaling pathways, which were enriched with gene sets associated with angiogenesis/vasculogenesis, embryonic development, and tissue and organ morphogenesis. Gene fusion transcripts were analyzed by various algorithms,[24,26] but recurrent fusions were not found in aSHH-MB.

## IHC With VEGFA Is a Tool for aSHH-MB Stratification

We selected *VEGFA* as a potential candidate for further clinically relevant stratification of aSHH-MB based on its high expression in MBII subgroup, known biological role,

**Table 3** Results of Univariate and Multivariate OS Analysis for 96 Adult SHH MB

| Variable | Uni-HR | *P*Value[a] | Multi-HR | *P*Value[a] |
|---|---|---|---|---|
| Age: < 35 years vs > 35 years | 0.32 | .77 | 0.98 | .96 |
| Gender: male vs female | 1.12 | .42 | 1.06 | .56 |
| Tumor location: median vs lateral | 0.88 | .34 | 0.96 | .94 |
| M stage: M0-1 vs M2-3 | 3.71 | .09 | 2.72 | .11 |
| Tumor resection: NTR vs GTR | 3.42 | .13 | 1.32 | .59 |
| *GLI2* amplification: yes vs no | **8.72** | **<.01** | 2.33 | .12 |
| Loss 9q: yes vs no | 0.59 | .43 | 0.97 | .98 |
| Loss 10q: yes vs no | **9.42** | **<.01** | 2.46 | .14 |
| Loss 17p: yes vs no | 2.11 | .184 | 1.82 | .28 |
| Loss 14q: yes vs no | 0.68 | .53 | 0.77 | .67 |
| Gain 3q: yes vs no | 0.57 | .31 | 0.41 | .14 |
| Balanced profile: yes vs no | 0.64 | .49 | 0.73 | .62 |
| *PTCH1* mutation: yes vs no | 0.93 | .38 | 0.98 | .42 |
| *SMO* mutation: yes vs no | 0.31 | .22 | 0.44 | .32 |
| *PRKAR1A* mutation: yes vs no | 0.34 | .28 | 0.57 | .44 |
| Molecular groups: aSHH-MBII vs MBI | **18.7** | **<.01** | **5.47** | **.02** |

**Abbreviations:** GTR, gross total tumor; NTR, near-total tumor; OS, overall survival.
[a]Log-rank test.
Bold value represent the significant differences.

and available antibody. *VEGFA* expression levels in aSHH-MBII were significantly higher than those for aSHH-MBI and pediatric SHH-MB ($P < .01$), but were quite comparable with those for MB-TP53, Group 3 and 4 MB (Figure 2C). Moreover, *VEGFA* expression levels were significantly higher for metastatic and lethal aSHH-MB and also for tumors harboring *GLI2* amplification and 10q loss (Supplementary Figure 3).

To test whether the expression of VEGFA is associated with survival, aSHH-MB samples were categorized as having "high" or "low" *VEGFA* mRNA levels using Bonferroni corrected multiple comparisons. These analyses showed that *VEGFA* expression with a *log2* RPKM cutoff > 2.5 was associated with aSHH-MBII cohort (28/76% of cases vs 5/14% for SHH-MBI; $P < .01$) and unfavorable aSHH-MB clinical outcomes in terms of PFS and OS (Figure 2D). In addition, *VEGFA* expression with cutoff > 2.5 was also associated with unfavorable outcomes for a whole pediatric SHH MB cohort (n = 100; Supplementary Figure 4), for children SHH MB (n = 27) but not for infant SHH MB (n = 73; data not shown).

Similar survival analyses of gene expression data generated with the Affymetrix platform for an independent set of SHH-MB (n = 103) also showed unfavorable outcomes for tumors with high *VEGFA* expression both in all SHH-MB and in aSHH-MB only (n = 47), thus confirming data obtained with the RNA sequencing platform (Supplementary Figure 5).

Next, we applied VEGFA monoclonal antibody (VG-1) to stain 74 aSHH-MB samples previously subjected to RNA-seq experiments (screening set) and the remaining 22 aSHH-MB samples for which only DNA methylation profiling was performed (validation set). The two following patterns of cytoplasmic VEGFA immunostaining were detected in a simple manner: (i) "Positive"—tumor sample was entirely and intensively stained (n = 33; Figure 2E). (ii) "Negative"—either patched, single collections of cells with heterogeneous staining intensity or no VEGFA expression was found throughout the entire sample (n = 41; Figure 2F). In the "screening set," samples with *VEGFA* gene expression over cutoff level were all positive (28/74% aSHH-MBII and 5/14% aSHH-MBI, respectively). Among the 22 aSHH-MB from the "validation set," PFS and OS differences were identified between 9 positive and 13 negative samples (log-rank test; $P < .01$; Supplementary Figure 6). When we analyzed survival for the entire aSHH-MB set (n = 96) with various degrees of VEGFA protein expression, we found that PFS and OS were significantly worse for patients harboring VEGFA-positive aSHH-MB (Figure 2G). Thus, the results of IHC evaluation corroborated the survival data obtained by transcriptome analysis.

We also tested VEGFA immunoexpression on iSHH-MB (n = 72) and cSHH-MB (n = 24) samples, where only 24% and 32%, respectively, were estimated as "positive." In addition, all 18 samples of SHH-MB53 were strongly positive as well as 82% of Group 3 and 74% of Group 4 MB (n = 97 and 112 samples, respectively).

## Discussion

Due to the low incidence of adult MB, no data exist regarding their optimal clinical stratification and management.[15,17,29] Recently, these patients are treated according to various protocols elaborated for treatment

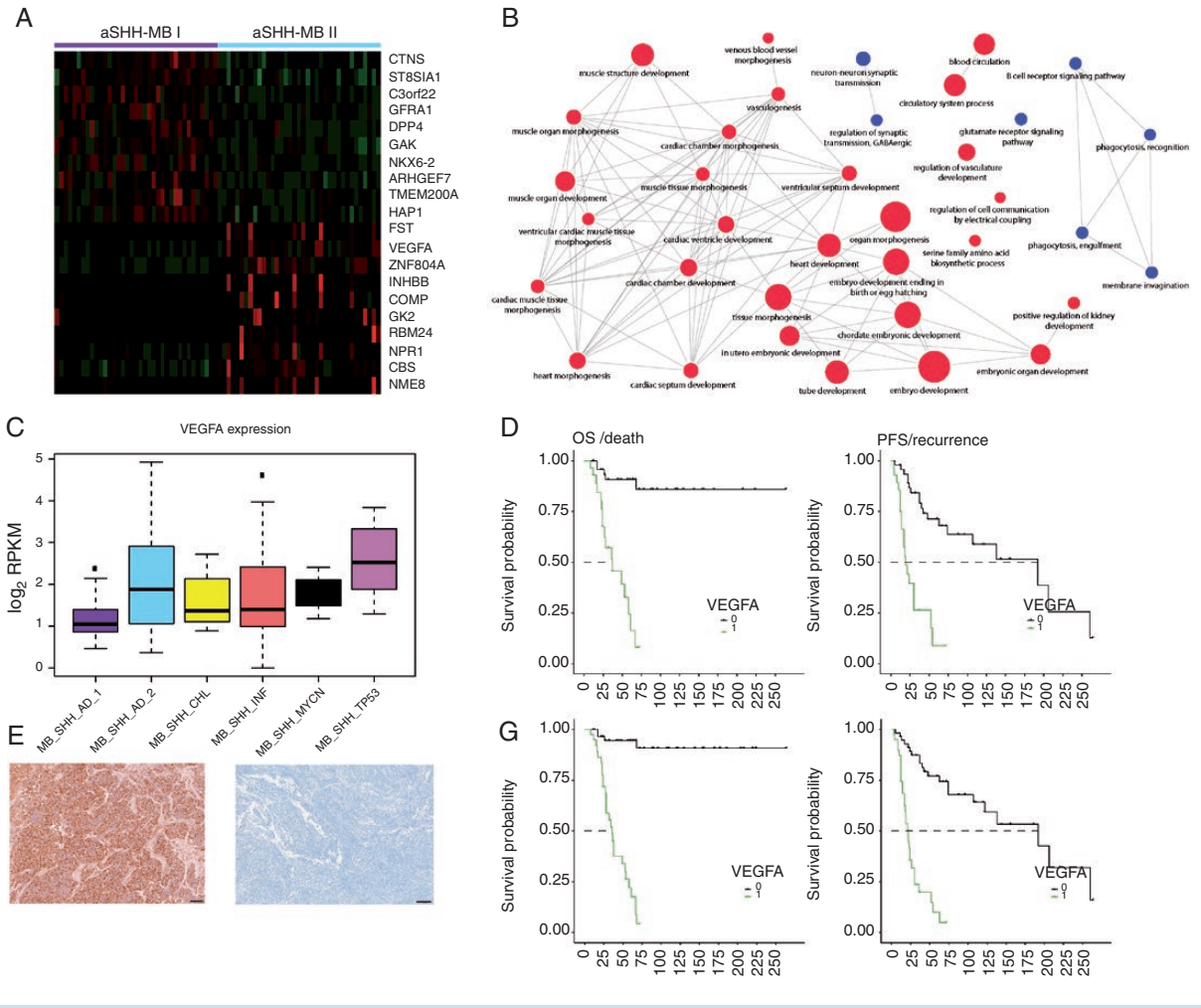


**Fig. 2** (A) A set of 20 top most-confident genes differentially overexpressed in aSHH-MBI (violet top line) and aSHH-MBII (blue top line), respectively, allows one to discriminate clearly between these tumor cohorts. (B) Gene Ontology analysis disclosed that aSHH-MBI RNA profiles (blue circles) were associated with neuronal metabolism, synaptic transmission, and phagocytosis. In contrast, expression profiling signatures of aSHH-MBII (red circles) were characterized by genes involved in angiogenesis, tissue morphogenesis, and embryonal development. (C) *VEGFA* expression level is significantly higher (Mann-Whitney *U* test, $P < .01$) in aSHH-MBII (blue boxplot; n = 38) in comparison to aSHH-MBI (violet boxplot; n = 36), children *TP53* wt SHH MB (orange boxplot; n = 16), infant SHH-MB (red boxplot; n = 73). However, *VEGFA* expression was also high in *TP53* mutant SHH MB (pink boxplot; n = 11). (D) Survival analysis for *VEGFA* expression in aSHH-MB shows that both overall survival (OS) and progression-free survival (PFS) were significantly worse for those with gene overexpression harboring *log2* Read per Million Kilobase (RPKM) > 2.5 (green line; log-rank test; $P < .01$). (E) Diffuse VEGFA immunoexpression in aSHH-MB allocated to MBII cohort (the scale bars: 50 µm). (F) Completely VEGFA-negative tumor sample with aSHH-MBI molecular signature (the scale bars: 50 µm). (G) Survival analysis for 96 aSHH-MB shows that both OS and PFS were significantly worse for patients harboring VEGFA immunopositive tumor samples (green line; log-rank test; $P < .01$).

of either pediatric MB or even glioblastomas.[30–34] Moreover, adult MB have been suspected to be different from their childhood counterparts in terms of clinical outcomes and tumor biology.[4–7,18–20,35] In contrast to pediatric patients with SHH-MB MB, for whom tumor relapses mostly occur locally, aSHH-MB patients disclosed variable patterns of relapses from slowly growing and successfully salvaged local recurrences to rapid and fatal metastatic spread.[14,17,28,30,31,34,36] It has been also recently found that SHH-MB diagnosed in infants, children, and adults strongly differ in mutational landscapes, epigenetic and gene expression profiles.[4,5,7,8,10] At least 4 molecular subtypes within SHH-MB have been identified with the SHHδ variant (strongly enriched for *TERT* promoter mutations) being most common in adults.[8,10] However, biological mechanisms underlying differences in the clinical courses between pediatric and adult MB, and survival heterogeneity within the aSHH-MB cohort are still unclear.

We molecularly analyzed a series of uniformly treated aSHH-MB and two distinct aSHH-MB epigenetic subsets of numerically comparable size were identified, which were associated with different patients' outcomes. These molecular subsets disclosed conspicuous variability in their cytogenetic profiles, mutational landscapes, and transcriptional programs.

Tumors from the aSHH-MBI subset were associated with *PTCH1/SMO* mutations, neurometabolic/neurotransmissive biological processes, and favorable outcomes. It suggests a benefit of HIT-based therapy for patients with the aSHH-MBI signature. However, some of aSHH-MBI tended to develop late local relapses thus requesting long-term post-treatment surveillance and/or salvage molecular therapy with SMO inhibitors, especially in cases harboring upstream SHH pathway mutations like *PTCH1*.[5,21]

Tumors from the aSHH-MBII molecular subset were enriched in *GLI2* amplifications and losses of 10q, which have been previously identified as "unfavorable" molecular patterns for SHH-MB.[3,6,10] These tumors disclosed "high mutational burden" and gene expression signatures associated with angiogenesis and embryonal development. The distinct biological mechanisms underlying an activation of different transcriptional programs in aSHH-MB remain to be defined. Perhaps, two outlined aSHH-MB molecular subsets have different cell(s) of origin and, therefore, single-cell transcriptome analysis would be useful to identify their cellular contents, sources, and developmental trajectories.[28]

Metastatic relapses (both CNS and extra-neural) were predominately diagnosed in aSHH-MBII patients receiving HIT-based radio-chemotherapy as a first-line treatment. Thus, it appears that tumor dissemination cannot be effectively prevented in these tumors by the standard radio-chemotherapy and it requests a development of their alternative treatment strategies. *VEGFA* is a key angiogenic mediator that is activated in CNS tumors including Group 3 MB where high level of VEGFA expression was associated with poor survival.[37] In the current study, *VEGFA* was identified among the top upregulated genes in aSHH-MBII subset and its' high expression both at mRNA and protein levels was associated with extremely poor outcomes. Given the clinical importance of aSHH-MBII identification, VEGFA IHC could be adopted to routine practice as a valid surrogate biomarker. High levels of *VEGFA* expression may be also considered as therapeutically targetable genetic driver for the treatment-resistant aSHH-MB and a potent application of anti-angiogenic therapy for these patients might require to be considered.[37–42]

In conclusion, the histologically uniform aSHH-MB cohort exhibits clear molecular heterogeneity separating these tumors into two clinically relevant subsets: prognostically favorable, "neuronal" aSHH-MBI and clinically aggressive, "embryonic" aSHH-MBII. VEGF-mediated angiogenesis may play a role in the pathogenesis of aSHH-MBII and VEGFA expression at RNA and/or protein level appears to be a reliable biomarker that could accurately predict clinical course and, perhaps, response to radio-chemotherapy.

## Supplementary Material

Supplementary material is available at *Neuro-Oncology* online.


## Keywords

adult | medulloblastoma | prognosis | SHH | transcriptome | VEGFA

## Funding

A.K. is supported by the Helmholtz Association Research Grant HRSF-0005 (Germany). M.R., A.G., and O.Zh. are supported by the Russian Scientific Foundation Research (RSF) Grant no. 18-45-06012 (Russia).

## Acknowledgments

The authors thank patients and their families/caregivers for their support. All authors were involved in the data gathering, analysis, review, interpretation, and manuscript preparation and approval.


**Conflict of interest statement.** There are no conflicts of interest for any authors.

**Authorship statement.** Experimental design: A.K., K.O., S.M.P., A.v.D., and M.K. Implementation: A.K., K.O., M.R., O.Zh., S.M.P., A.v.D., and M.K. Data analysis/interpretation: all authors. Sample collection: A.K., M.R., O.A., O.Zh., and A.G. Manuscript writing: all authors. Final approval of manuscript: all authors. Accountable for all aspects of the study: all authors.

## References


1. Ang C, Hauerstock D, Guiot MC, et al. Characteristics and outcomes of medulloblastoma in adults. *Pediatr Blood Cancer.* 2008;51(5):603–607.
2. Atalar B, Ozsahin M, Call J, et al. Treatment outcome and prognostic factors for adult patients with medulloblastoma: the Rare Cancer Network (RCN) experience. *Radiother Oncol.* 2018;127(1):96–102.
3. Smoll NR. Relative survival of childhood and adult medulloblastomas and primitive neuroectodermal tumors (PNETs). *Cancer.* 2012;118(5):1313–1322.
4. Al-Halabi H, Nantel A, Klekner A, et al. Preponderance of sonic hedgehog pathway activation characterizes adult medulloblastoma. *Acta Neuropathol.* 2011;121(2):229–239.
5. Kool M, Jones DT, Jäger N, et al.; ICGC PedBrain Tumor Project. Genome sequencing of SHH medulloblastoma predicts genotype-related response to smoothened inhibition. *Cancer Cell.* 2014;25(3):393–405.
6. Kool M, Korshunov A, Remke M, et al. Molecular subgroups of medulloblastoma: an international meta-analysis of transcriptome,

genetic aberrations, and clinical data of WNT, SHH, Group 3, and Group 4 medulloblastomas. *Acta Neuropathol.* 2012;123(4):473–484.
7. Northcott PA, Hielscher T, Dubuc A, et al. Pediatric and adult sonic hedgehog medulloblastomas are clinically and molecularly distinct. *Acta Neuropathol.* 2011;122(2):231–240.
8. Cavalli FMG, Remke M, Rampasek L, et al. Intertumoral heterogeneity within medulloblastoma subgroups. *Cancer Cell.* 2017;31(6):737–754. e6.
9. Mynarek M, von Hoff K, Pietsch T, et al. Nonmetastatic medulloblastoma of early childhood: results from the prospective clinical trial HIT-2000 and an extended validation cohort. *J Clin Oncol.* 2020;38(18):2028–2040.
10. Northcott PA, Buchhalter I, Morrissy AS, et al. The whole-genome landscape of medulloblastoma subtypes. *Nature.* 2017;547(7663):311–317.
11. Robinson GW, Rudneva VA, Buchhalter I, et al. Risk-adapted therapy for young children with medulloblastoma (SJYC07): therapeutic and molecular outcomes from a multicentre, phase 2 trial. *Lancet Oncol.* 2018;19(6):768–784.
12. Schwalbe EC, Lindsey JC, Nakjang S, et al. Novel molecular subgroups for clinical classification and outcome prediction in childhood medulloblastoma: a cohort study. *Lancet Oncol.* 2017;18(7):958–971.
13. Brandes AA, Bartolotti M, Marucci G, et al. New perspectives in the treatment of adult medulloblastoma in the era of molecular oncology. *Crit Rev Oncol Hematol.* 2015;94(3):348–359.
14. Beier D, Proescholdt M, Reinert C, et al. Multicenter pilot study of radiochemotherapy as first-line treatment for adults with medulloblastoma (NOA-07). *Neuro Oncol.* 2018;20(3):400–410.
15. Franceschi E, Hofer S, Brandes AA, et al. EANO-EURACAN clinical practice guideline for diagnosis, treatment, and follow-up of postpubertal and adult patients with medulloblastoma. *Lancet Oncol.* 2019;20(12):e715–e728.
16. Majd N, Penas-Prado M. Updates on management of adult medulloblastoma. *Curr Treat Options Oncol.* 2019;20(8):64.
17. Penas-Prado M, Theeler BJ, Cordeiro B, et al. Proceedings of the comprehensive oncology network evaluating rare CNS tumors (NCI-CONNECT) adult medulloblastoma workshop. *Neurooncol Adv.* 2020;2(1):vdaa097.
18. Kool M, Korshunov A, Pfister SM. Update on molecular and genetic alterations in adult medulloblastoma. *Memo.* 2012;5(3):228–232.
19. Wong GC, Li KK, Wang WW, et al. Clinical and mutational profiles of adult medulloblastoma groups. *Acta Neuropathol Commun.* 2020;8(1):191.
20. Zhao F, Ohgaki H, Xu L, et al. Molecular subgroups of adult medulloblastoma: a long-term single-institution study. *Neuro Oncol.* 2016;18(7):982–990.
21. Li Y, Song Q, Day BW. Phase I and phase II sonidegib and vismodegib clinical trials for the treatment of paediatric and adult MB patients: a systemic review and meta-analysis. *Acta Neuropathol Commun.* 2019;7(1):123.
22. Hovestadt V, Remke M, Kool M, et al. Robust molecular subgrouping and copy-number profiling of medulloblastoma from small amounts of archival tumour material using high-density DNA methylation arrays. *Acta Neuropathol.* 2013;125(6):913–916.
23. Capper D, Jones DTW, Sill M, et al. DNA methylation-based classification of central nervous system tumours. *Nature.* 2018;555(7697):469–474.
24. Korshunov A, Okonechnikov K, Sahm F, et al. Transcriptional profiling of medulloblastoma with extensive nodularity (MBEN) reveals two clinically relevant tumor subsets with VSNL1 as potent prognostic marker. *Acta Neuropathol.* 2020;139(3):583–596.
25. Bindea G, Mlecnik B, Hackl H, et al. ClueGO: a Cytoscape plug-in to decipher functionally grouped gene ontology and pathway annotation networks. *Bioinformatics.* 2009;25(8):1091–1093.
26. Okonechnikov K, Imai-Matsushima A, Paul L, Seitz A, Meyer TF, Garcia-Alcalde F. InFusion: advancing discovery of fusion genes and chimeric transcripts from deep RNA-sequencing data. *PLoS One.* 2016;11(12):e0167417.
27. Louis DN, Ohgaki H, Wiestler OD, et al., eds. *WHO Classification of Tumours of the Central Nervous System.* IARC Press; 2016.
28. Hovestadt V, Smith KS, Bihannic L, et al. Resolving medulloblastoma cellular architecture by single-cell genomics. *Nature.* 2019;572(7767):74–79.
29. De B, Beal K, De Braganca KC, et al. Long-term outcomes of adult medulloblastoma patients treated with radiotherapy. *J Neurooncol.* 2018;136(1):95–104.
30. Friedrich C, von Bueren AO, von Hoff K, et al. Treatment of adult nonmetastatic medulloblastoma patients according to the paediatric HIT 2000 protocol: a prospective observational multicentre study. *Eur J Cancer.* 2013;49(4):893–903.
31. Kann BH, Lester-Coll NH, Park HS, et al. Adjuvant chemotherapy and overall survival in adult medulloblastoma. *Neuro Oncol.* 2017;19(2):259–269.
32. Kocakaya S, Beier CP, Beier D. Chemotherapy increases long-term survival in patients with adult medulloblastoma – a literature-based meta-analysis. *Neuro Oncol.* 2016;18(3):408–416.
33. von Bueren AO, Friedrich C, von Hoff K, et al. Metastatic medulloblastoma in adults: outcome of patients treated according to the HIT2000 protocol. *Eur J Cancer.* 2015;51(16):2434–2443.
34. Mokhtech M, Morris CG, Indelicato DJ, Rutenberg MS, Amdur RJ. Patterns of failure in patients with adult medulloblastoma presenting without extraneural metastasis. *Am J Clin Oncol.* 2018;41(10):1015–1018.
35. Remke M, Hielscher T, Northcott PA, et al. Adult medulloblastoma comprises three major molecular variants. *J Clin Oncol.* 2011;29(19):2717–2723.
36. Ramaswamy V, Remke M, Bouffet E, et al. Recurrence patterns across medulloblastoma subgroups: an integrated clinical and molecular analysis. *Lancet Oncol.* 2013;14(12):1200–1207.
37. Thompson EM, Keir ST, Venkatraman T, et al. The role of angiogenesis in Group 3 medulloblastoma pathogenesis and survival. *Neuro Oncol.* 2017;19(9):1217–1227.
38. Aguilera D, Mazewski C, Fangusaro J, et al. Response to bevacizumab, irinotecan, and temozolomide in children with relapsed medulloblastoma: a multi-institutional experience. *Childs Nerv Syst.* 2013;29(4):589–596.
39. Bonney PA, Santucci JA, Maurer AJ, Sughrue ME, McNall-Knapp RY, Battiste JD. Dramatic response to temozolomide, irinotecan, and bevacizumab for recurrent medulloblastoma with widespread osseous metastases. *J Clin Neurosci.* 2016;26:161–163.
40. Peyrl A, Chocholous M, Kieran MW, et al. Antiangiogenic metronomic therapy for children with recurrent embryonal brain tumors. *Pediatr Blood Cancer.* 2012;59(3):511–517.
41. Schiavetti A, Varrasso G, Mollace MG, et al. Bevacizumab-containing regimen in relapsed/progressed brain tumors: a single-institution experience. *Childs Nerv Syst.* 2019;35(6):1007–1012.
42. Korshunov A, Remke M, Werft W, et al. Adult and pediatric medulloblastomas are genetically distinct and require different algorithms for molecular risk stratification. *J Clin Oncol.* 2010;28(18):3054–3060.